Multi-focus parallel detection of fluorescent molecules at picomolar concentration with photonic nanojets arrays

P. Ghenuche, J. De Torres, P. Ferrand, J. Wenger

Multi-focus parallel detection of fluorescent molecules at picomolar concentration with photonic nanojets arrays

Petru Ghenuche, Juan de Torres, Patrick Ferrand, and Jérôme Wenger

Citation: Applied Physics Letters **105**, 131102 (2014); doi: 10.1063/1.4896852
View online: http://dx.doi.org/10.1063/1.4896852
View Table of Contents: http://scitation.aip.org/content/aip/journal/apl/105/13?ver=pdfcov
Published by the AIP Publishing

Multi-focus parallel detection of fluorescent molecules at picomolar concentration with photonic nanojets arrays

Petru Ghenuche,[a] Juan de Torres, Patrick Ferrand, and Jérôme Wenger[b]
CNRS, Aix Marseille Université, Ecole Centrale Marseille, Institut Fresnel UMR7249, 13013 Marseille, France

(Received 4 September 2014; accepted 19 September 2014; published online 29 September 2014)

Fluorescence sensing and fluorescence correlation spectroscopy (FCS) are powerful methods to detect and characterize single molecules; yet, their use has been restricted by expensive and complex optical apparatus. Here, we present a simple integrated design using a self-assembled bi-dimensional array of microspheres to realize multi-focus parallel detection scheme for FCS. We simultaneously illuminate and collect the fluorescence from several tens of microspheres, which all generate their own photonic nanojet to efficiently excite the molecules and collect the fluorescence emission. Each photonic nanojet contributes to the global detection volume, reaching FCS detection volumes of several tens of femtoliters while preserving the fluorescence excitation and collection efficiencies. The microspheres photonic nanojets array enables FCS experiments at low picomolar concentrations with a drastic reduction in apparatus cost and alignment constraints, ideal for microfluidic chip integration. © *2014 AIP Publishing LLC*.
[http://dx.doi.org/10.1063/1.4896852]

The ability to detect fluorescent molecules in solution is a core technology for biochemical assays,[1] flow cytometry,[2] and fluorescence correlation spectroscopy (FCS).[3] To reach the ultimate level of single molecule sensitivity, it is crucial to simultaneously maximize the fluorescence collection efficiency and minimize the background.[4] Therefore, most instruments are built around a confocal microscope equipped with a high numerical aperture objective. However, the cost of this apparatus, its complexity, and the constraints on optical alignment have limited the implementation of single molecule fluorescence spectroscopy outside the research laboratories.

Several approaches have been proposed to avoid the use of the high NA objective and realize integrated devices with single molecule sensitivity.[5] These include plastic aspheric lenses,[6,7] compact single-lens systems,[8] supercritical angle collection lenses,[9,10] optical fibers,[11–13] microlenses arrays,[14] and polystyrene microspheres.[15–17] Microspheres appear especially attractive because of their excellent focusing ability, low intrinsic cost, and large commercial availability. Under collimated illumination, the beam that emerges from the microsphere has high intensity, subwavelength transverse dimensions, and low divergence, and was therefore termed photonic nanojet.[18–20] This focusing property has led to several successes in light confinement,[21–23] guiding,[24] and imaging.[25] However, two issues challenge the use of single microsphere lenses for fluorescence detection.[15–17] First, it requires careful positioning of the microsphere respective to the objective lens. Second, the relatively small confocal volume of 1 fL with a 2 μm sphere sets a lower limit of 200 pM so as to detect an average of 0.1 molecule in the confocal volume.[15] Reaching lower concentrations to detect traces of fluorescent analytes requires an enlarged detection volume. However, using a microsphere of larger diameter is not a relevant option, as the larger volume comes along a drastically degraded signal-to-noise ratio for fluorescence detection.

Here, we present a design using a self-assembled bi-dimensional array of microspheres to realize multi-focus parallel detection of fluorescent molecules and FCS. Instead of using a single microsphere as in earlier works,[15,16] here, we simultaneously illuminate and collect the fluorescence from several tens of microspheres (Fig. 1). A low NA objective is used to illuminate a zone of 10 μm width, covering a large number of microspheres which all generate their own photonic nanojet to efficiently excite the molecules and collect the fluorescence emission. The fluorescence light from the whole zone is then sent to a large surface photon counting module whose single output is analyzed by FCS correlation analysis. This design circumvents the aforementioned limitations. As large areas are involved, the method has less stringent alignment requirements and does not demand expensive positioning tools. As several tens of microspheres contribute to focus the light, the global effective detection volume is large while a high fluorescence collection efficiency is maintained. This realizes a regime of parallel detection of single fluorescent molecules in a multi-focus environment and enables FCS experiments at low picomolar concentrations. Moreover, the homogeneous arrays of microspheres are quite easy to obtain and have the potential for integration into microfluidic chambers, resulting in a disposable cost-efficient device with easy and robust operation.

The design of the system is illustrated in Fig. 1(a). Latex microspheres of calibrated 2 μm diameter, 1.59 refractive index, and dispersion smaller than 0.1% are diluted in pure water and dispersed on a quartz microscope coverslip. During water evaporation, the spheres self-assemble in a hexagonal lattice of several tens of μm^2 (Fig. 1(c)). Additionally, more advanced techniques could be applied to increase the array area.[26]

[a]On leave from Institute for Space Sciences, Bucharest-Măgurele RO-077125, Romania.
[b]Electronic mail: jerome.wenger@fresnel.fr

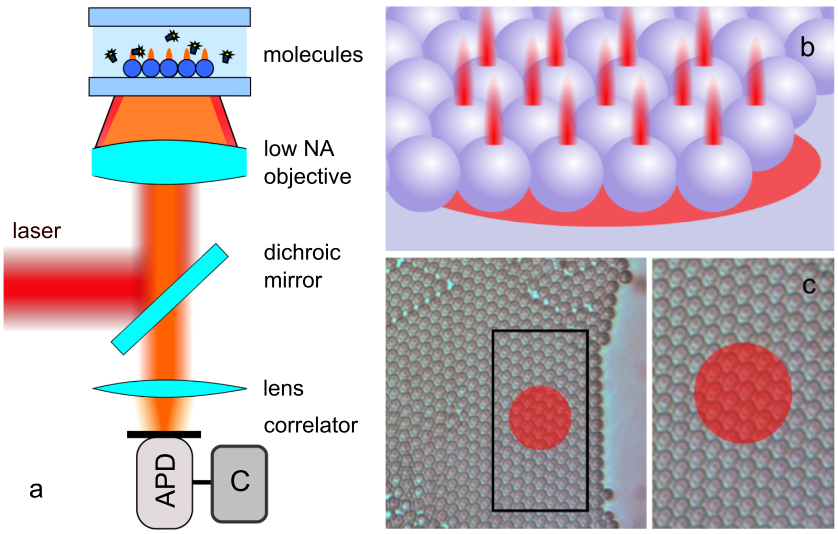

FIG. 1. (a) Experimental FCS configuration. (b) Scheme of the parallel multi-focus detection. (c) Microscope image of the microspheres array (inset: zoom of the indicated area in black rectangle). The microspheres diameter is 2 μm. The zone illuminated by the laser light is indicated by the red circle.

The parallel detection scheme proposed here strongly relies on the ability to carefully design and control the light distribution around several tens of microspheres, ensuring a high quality photonic jet for each sphere. The electromagnetic field distribution in the vicinity of microspheres was computed using a 3D finite-difference time-domain method (FDTD) (Rsoft Fullwave 6.0 commercial software) when illuminated with a Gaussian beam with a full width at half maximum of 10.0 μm corresponding to the experimental conditions (Fig. 2). Only one layer of focal spots, close to the spheres has a significant intensity and will contribute the most to the signal.

The array of microspheres is inserted in a microchamber made with two quartz coverslips separated by a 30 μm spacer. The microchamber is then filled with the water solution containing the fluorescent dyes at concentrations calibrated with absorption spectroscopy and FCS in conventional confocal setups. The experiments are performed with a low 0.3 NA objective and 10× magnification to illuminate an area of 10.5 μm diameter containing about 25 microspheres. No positioning system apart the microscope translation stage was used. This constitutes a major technical improvement as compared to earlier works, which required a 3D piezoelectric nanopositioning stage.[15,17] The linearly polarized laser excitation source is provided by a continuous He-Ne laser at 633 nm or a tunable picosecond laser (iChrome-TVIS, Toptica GmbH). The fluorescence is collected with the same 10× 0.3 NA objective, filtered from the scattered laser light by a dichroic mirror and focused on an avalanche photodiode (Perkin-Elmer SPCM-AQR-13, 175 μm active area) with 670 ± 20 nm bandpass filters. To perform FCS, the Transistor-Transistor Logic (TTL) output of the photodiode is analyzed by a hardware correlator (ALV-GmbH ALV6000) or a fast time-correlated single photon counting module (Hydraharp400, Picoquant GmbH).

FCS is based on computing the second order correlation function $g^{(2)}(\tau)$ of the fluorescence intensity $F(t)$ as function of the lag time τ : $g^{(2)}(\tau) = \langle F(t) \times F(t+\tau)\rangle / \langle F(t)\rangle^2$. In our microspheres array configuration, the fluorescence intensity is the sum of the individual fluorescence signals $F_i(t)$ generated by n photonic nanojets: $F(t) = \sum_{i=1}^{n} F_i(t)$. Therefore, the second order correlation function can be written as

$$g^{(2)}(\tau) = \frac{1}{\langle F\rangle^2} \times \left[\sum_{i=j} \langle F_i(t) \times F_j(t+\tau)\rangle + \sum_{i\neq j} \langle F_i(t) \times F_j(t+\tau)\rangle \right]. \quad (1)$$

This expression can be simplified if we assume that all n photonic nanojets are equivalent

$$g^{(2)}(\tau) = \frac{1}{n} \times \frac{\langle F_i(t) \times F_i(t+\tau)\rangle}{\langle F_i\rangle^2} + \sum_{i\neq j} \frac{\langle F_i(t) \times F_j(t+\tau)\rangle}{\langle F\rangle^2}. \quad (2)$$

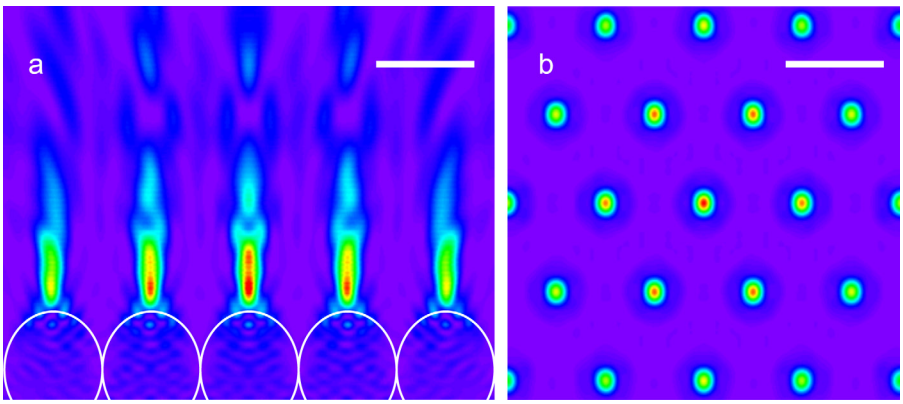

FIG. 2. 3D FDTD-calculated electric field intensity of the monolayer of microspheres illuminated by a Gaussian beam of 10 μm FWHM at $\lambda = 633$ nm. (a) XZ vertical cut. (b) XY horizontal cut at the plane of maximum intensity. The scale bar is 2 μm.

The first term corresponds to the autocorrelation $g^{(2)}_{AC,i}(\tau) = \langle F_i(t) \times F_i(t+\tau)\rangle / \langle F_i\rangle^2$ obtained for *one* photonic nanojet divided by the number of nanojets. The second term relates to spatial cross-correlation $g^{(2)}_{CC}(\tau)$ between different focal spots. It corresponds to the probability of finding the molecule in another nanojet at a given lag time τ given the fact that the molecule is present in one nanojet at $\tau = 0$.

The fluorescence autocorrelation for one photonic nanojet can be written following the classical analytical formula for FCS accounting for triplet blinking[3,15]

$$g^{(2)}_{AC,i}(\tau) = \frac{1}{N_i} \times \frac{1 + n_T \times \exp(-\tau/\tau_T)}{(1+\tau/\tau_d) \times \sqrt{1 + s^2\,\tau/\tau_d}}, \qquad (3)$$

where N_i is the number of molecules found in one photonic nanojet, n_T is the amplitude of the dark state population, and τ_T is the dark state blinking time. $\tau_d = w_0^2/4D$ is the mean diffusion time to cross one photonic jet of transverse waist w_0. D is the translational diffusion coefficient of the molecule under study. s is the ratio of transversal to axial dimensions of the analysis volume, which is set to $s = 0.2$ according to numerical simulations (Fig. 2) and previous work.[15]

The spatial cross-correlation term $g^{(2)}_{CC}(\tau)$ between two neighboring focal spots is deduced from earlier works on two-focus Fluorescence Cross Correlation Spectroscopy (FCCS) in the limiting case where no flow is present[27–29]

$$g^{(2)}_{CC}(\tau) = \beta \times g^{(2)}_{AC,i}(\tau) \times \exp\left[-\frac{R^2}{w_0^2} \times \frac{1}{1+\tau/\tau_d}\right], \qquad (4)$$

R is the distance between focal spots which equals here the microspheres diameter, and β is a constant prefactor that we keep as free parameter during the fits. To keep the analysis simple, we neglect cross-correlation terms between non-neighboring spots as they have a vanishing influence on the FCS trace. If desired, such terms could be included based on Eq. (4).

An important point to stress is that the cross-correlation term $g^{(2)}_{CC}(\tau)$ vanishes for short lag times $\tau \to 0$ as the distance R between neighboring spots is always significantly larger than the spot's transverse dimension w_0. Hence, for lag times below the translational diffusion time through one nanojet $\tau < \tau_d$, the total correlation function from the microspheres array can be safely approximated by the collection of individual autocorrelation terms

$$g^{(2)}(\tau) \simeq \frac{g^{(2)}_{AC,i}(\tau)}{n}. \qquad (5)$$

Notably, the amplitude of the correlation function near zero lag time is directly inversely proportional to the total number of detected molecules $N = n \times N_i$ in all the illuminated photonic nanojets. This expression clearly shows that multiple focal spots can be used simultaneously to detect the presence of fluorescent molecules and that FCS can be directly used to quantify the total number of molecules present in all the focal spots. The microspheres array configuration is thus conceptually similar to standard FCS with a large confocal volume.

We assess the potential of our parallel detection scheme by comparing the FCS results for the microspheres array to the classical confocal configuration, taken with a $63\times$ 1.2 NA water-immersion objective with a confocal volume of 0.5 fL (Fig. 3). Identical Alexa Fluor 647 solution at 7 nM was used for both measurements. The critical parameters obtained after the numerical analysis of the FCS data are indicated in the figure caption. For both measurements we observe a main feature of $g^2(\tau)$, which corresponds to the autocorrelation term. The confocal and the microspheres array show similar diffusion times τ_d, indicating the tight focusing induced by the photonic nanojet down to a transverse dimension of $w_0 = 275$ nm (calibrated from the known diffusion coefficient of Alexa Fluor 647 (Ref. 30)). In the case of the microspheres array, it is interesting to note the broad feature at longer lag times that we attribute to the cross-correlation term $g^{(2)}_{CC}(\tau)$ through several nanojets.[27–29] The numerical fit of the FCS data converges to a distance between neighboring spots of $R = 2.05\,\mu$m, in remarkable agreement with the microspheres diameter.

Next, we vary the concentration of the fluorescent dyes between 20 pM and 16 nM. A linear behavior of the number of molecules is observed even for low concentrations in the picomolar regime (Figs. 4(a) and 4(b)). Currently, we estimate that the sensitivity of our apparatus is around 10 pM, limited by the background luminescence noise. From the slope of the curve in Fig. 4(b), we estimate the effective volume associated with the microspheres array $V_{eff} \approx 30$ fL. This volume is

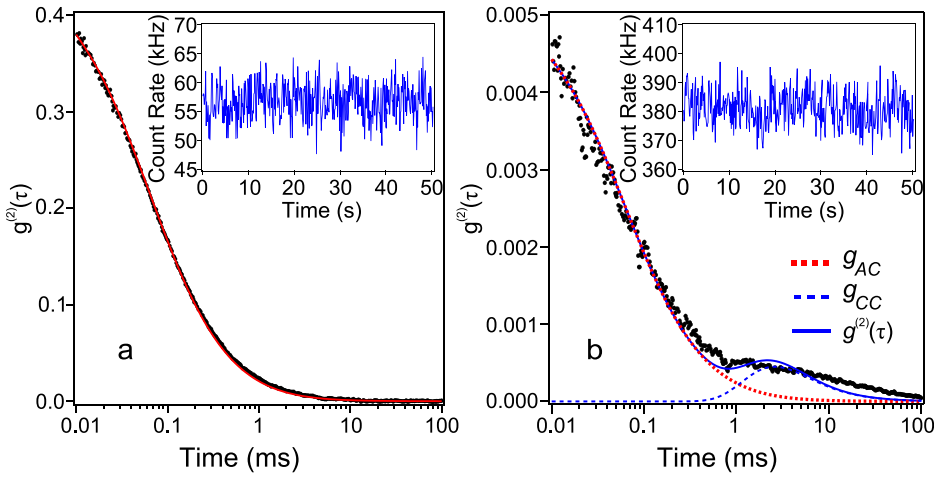

FIG. 3. Correlation functions recorded for the confocal reference (a) and the microspheres array (b) using identical 7 nM Alexa Fluor 647 solution (dots: are FCS data and lines are numerical fits). FCS fits results for the confocal reference: $N = 2.23$, $\tau_D = 64\,\mu$s, $n_T = 0.6$, $\tau_T = 2\,\mu$s; for the microspheres array: $N = 158$, $\tau_D = 63\,\mu$s, $n_T = 0.76$, $\tau_T = 2\,\mu$s, $\beta = 22.5$, $R = 2.05\,\mu$m, and $w_0 = 275$ nm. Insets: raw fluorescence timetraces.

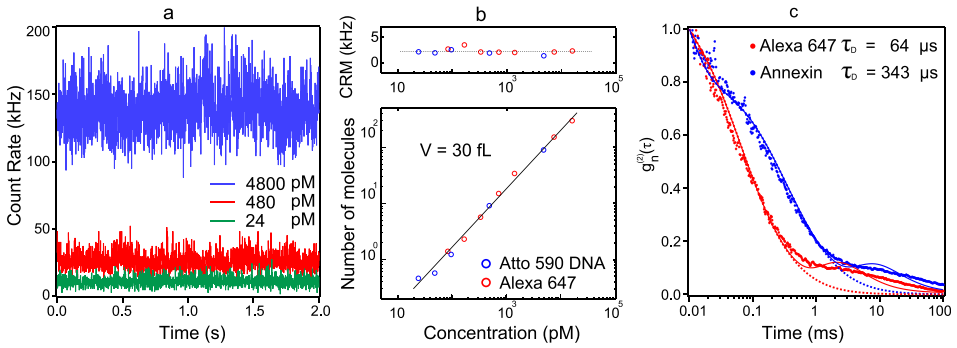

FIG. 4. (a) Raw fluorescence time traces recorded with the microspheres array for three characteristic concentrations of Atto590. (b) Number of molecules N from the FCS measurements versus the solution concentration for two different fluorescent dyes: Alexa Fluor 647 (red) and Atto590 (blue). The inset on top shows the constant count rate per molecule ($CRM = F/N$) as the concentration is varied. (c) Normalized correlation functions recorded for Alexa Fluor 647 (red) and Annexin A5b labeled with Cyanine-5 (blue). Dots are FCS data, solid lines are numerical fits according to Eq. (2), and dotted lines are numerical fits using only the single spot autocorrelation model of Eq. (5).

about 30× the volume of the nanojet generated by a single microsphere,[15] close to the expected number of 25 microspheres of 2 μm diameter illuminated by a 10 μm wide spot (Fig. 1(c)). We have also performed additional experiments where we vary the size of the incoming laser beam to illuminate a different number of microspheres. To summarize our results, the detection volume scales with the number n of illuminated spheres, each microsphere's nanojet contributing to a volume of ~1 fL. Altogether, these measurements confirm the multi-focus parallel detection of fluorescent molecules, each photonic nanojet contributing to the global detection volume. This provides a practical way to reach detection volumes of several tens of femtoliters while preserving the fluorescence excitation and collection efficiencies.

In addition to the concentration measurements, our technique is also able to distinguish between different fluorescent molecules based on their diffusion properties. To demonstrate this feature, we have measured the cellular protein Annexin A5b labeled with the Cyanine 5 fluorescent dye. Annexin A5b is a 36 kDa protein of 2.8 nm hydrodynamic radius, 4.5× larger than the radius for Alexa Fluor 647.[30] The FCS measurements on microspheres arrays report an increase in diffusion time from 64 μs for Alexa 647 to 343 μs for Annexin A5b (Fig. 4(c)), in agreement with the expected increase in hydrodynamic radius. This confirms the FCS capabilities of the microspheres array.

To conclude, we report the parallel detection of fluorescent molecules in a multi-focus photonic nanojets environment created by an array of microspheres. Each photonic nanojet contributes to the global detection volume, enabling FCS detection volumes of several tens of femtoliters while preserving the fluorescence excitation and collection efficiencies. Replacing the high NA microscope objective by the microspheres array greatly reduces the cost to the level of a disposable component which can be integrated into more complex microfluidic devices. The large areas involved in this design greatly relax the alignment constraints and avoid the use of expensive positioning stages. As additional advantage of our design, the relatively short diffusion time needed for the fluorescent molecule to cross the analysis volume limits observing the negative effects of photobleaching. We have demonstrated that this inexpensive method can be used to detect fluorescent compounds down to concentrations in the picomolar range, and assess various molecular parameters such as fluorescence brightness, photophysical blinking, diffusion coefficient, or relative hydrodynamic radius.

The research leading to these results has received funding from the European Commission's Seventh Framework Programme (FP7-ICT-2011-7) under grant agreement ERC StG 278242 (ExtendFRET).

[1]M. Sauer, K. H. Drexhage, C. Zander, and J. Wolfrum, Chem. Phys. Lett. **254**, 223 (1996).
[2]M. Eigen and R. Rigler, Proc. Natl. Acad. Sci. U. S. A. **91**, 5740 (1994).
[3]S. Maiti, U. Haupts, and W. W. Webb, Proc. Natl. Acad. Sci. U. S. A. **94**, 11753 (1997).
[4]R. Rigler, Ü. Mets, J. Widengren, and P. Kask, Eur. Biophys. J. **22**, 169 (1993).
[5]J. Wenger and H. Rigneault, Int. J. Mol. Sci. **11**, 206 (2010).
[6]T. Sonehara, T. Anazawa, and K. Uchida, Anal. Chem. **78**, 8395 (2006).
[7]E. Olson, R. Torres, and M. J. Levene, Biomed. Opt. Express **4**, 1074 (2013).
[8]N. K. Singh, J. V. Chacko, V. K. A. Sreenivasan, S. Nag, and S. Maiti, J. Biomed. Opt. **16**, 025004 (2011).
[9]T. Ruckstuhl, J. Enderlein, S. Jung, and S. Seeger, Anal. Chem. **72**, 2117 (2000).
[10]J. Ries, T. Ruckstuhl, D. Verdes, and P. Schwille, Biophys. J. **94**, 221 (2008).
[11]K. Garai, M. Muralidhar, and S. Maiti, Appl. Opt. **45**, 7538 (2006).
[12]P. Haas, P. Then, A. Wild, W. Grange, S. Zorman, M. Hegner, M. Calame, U. Aebi, J. Flammer, and B. Hecht, Anal. Chem. **82**, 6299 (2010).
[13]H. Aouani, F. Deiss, J. Wenger, P. Ferrand, N. Sojic, and H. Rigneault, Opt. Express **17**, 19085 (2009).
[14]A. Orth and K. B. Crozier, Opt. Express **22**, 18101 (2014).
[15]J. Wenger, D. Gérard, H. Aouani, and H. Rigneault, Anal. Chem. **80**, 6800 (2008).
[16]J. J. Schwartz, S. Stavrakis, and S. R. Quake, Nat. Nanotechnol. **5**, 127 (2010).
[17]D. Gérard, A. Devilez, H. Aouani, B. Stout, N. Bonod, J. Wenger, E. Popov, and H. Rigneault, J. Opt. Soc. Am. B **26**, 1473 (2009).
[18]Z. Chen, A. Taflove, and V. Backman, Opt. Express **12**, 1214 (2004).
[19]X. Li, Z. Chen, A. Taflove, and V. Backman, Opt. Express **13**, 526 (2005).
[20]A. Heifetz, S. C. Kong, A. V. Sahakian, A. Taflove, and V. Backman, J. Comput. Theor. Nanosci. **6**, 1979 (2009).
[21]P. Ferrand, J. Wenger, M. Pianta, H. Rigneault, A. Devilez, B. Stout, N. Bonod, and E. Popov, Opt. Express **16**, 6930 (2008).
[22]M. S. Kim, T. Scharf, S. Muhlig, C. Rockstuhl, and H. P. Herzig, Appl. Phys. Lett. **98**, 191114 (2011).
[23]A. Darafsheh, A. Fardad, N. M. Fried, A. N. Antoszyk, H. S. Ying, and V. N. Astratov, Opt. Express **19**, 3440 (2011).
[24]S. Yang and V. N. Astratov, Appl. Phys. Lett. **92**, 261111 (2008).
[25]A. Darafsheh, G. F. Walsh, L. D. Negro, and V. N. Astratov, Appl. Phys. Lett. **101**, 141128 (2012).

[26]M. Grzelczak, J. Vermant, E. M. Furst, and L. M. Liz-Marzan, ACS Nano **4**, 3591 (2010).
[27]M. Brinkmeier, K. Dörre, J. Stephan, and M. Eigen, Anal. Chem. **71**, 609 (1999).
[28]P. S. Dittrich and P. Schwille, Anal. Chem. **74**, 4472 (2002).
[29]T. Dertinger, V. Pacheco, I. von der Hocht, R. Hartmann, I. Gregor, and J. Enderlein, Chem. Phys. Chem. **8**, 433 (2007).
[30]P. Ghenuche, H. Rigneault, and J. Wenger, Opt. Express **20**, 28379 (2012).